

A Butterfly-Shaped Amphiphilic Molecule: Solution-Transferable and Free-Standing Bilayer Films for Organic Transistors**

Jie Yin, Yan Zhou, Ting Lei, and Jian Pei*

Ordered crystalline films are one of the most important elements in high-performance optoelectronic devices.^[1] Specially treated substrates and slow growth speeds are employed to produce such films by enlarging the grain size and reducing the grain boundaries. However, highly ordered crystalline films are difficult to lift off and transfer because of the strong interactions between the materials and the substrates.^[2] Expensive substrates and low compatibility of the special treatment constantly limit their applications in optoelectronic devices. Recently, free-standing films were fabricated on one substrate and transferred to a medium and placed onto the desired substrate to produce the final devices.^[3] Such separation of the film growth and device assembling process can significantly decrease the cost without sacrificing the performance of the devices. However, special substrates and lift-off processes were needed in these cases. Substrate-free formation of the self-assembled organic films is thus still challenging.

Organic nano- and microstructural materials, especially those self-assembled from π -conjugated molecules, have exhibited potential applications in electronic and photonic devices owing to their unique optoelectronic properties.^[4,5] Although various organic semiconductor devices from single molecules to bulky single crystals were fabricated,^[6] ordered free-standing 2D architectures and their device performances were rarely reported. A variety of novel supramolecular architectures can be created from amphiphilic molecules,^[7,8] however, the carrier transport properties of such assemblies have seldom been investigated. Herein, we report a free-standing film which was directly self-assembled in solution by a butterfly-shaped amphiphilic benzodithiophene derivative through strong π - π interactions between rigid aromatic cores and van der Waals interactions from both alkyl-alkyl and triethylene glycol (TEG) chains. Organic field-effect transistors incorporating such 2D free-standing films as the active layer are fabricated by a solution transfer process. The hole mobility in the transistors is up to $0.02 \text{ cm}^2 \text{ V}^{-1} \text{ s}^{-1}$. To the best of our knowledge, this is the first report of an organic

transistor based on a free-standing film which was directly self-assembled from solution without the assistance of a substrate.

Scheme 1 illustrates the synthetic approach to amphiphilic butterfly-shaped benzodithiophene derivative **1**. This amphiphilic molecule has a rigid aromatic backbone with alternating benzene and thiophene units that are peripherally substituted with two hydrophobic dodecyloxy chains and two hydrophilic TEG chains on the opposite sides. A FeCl_3 oxidative cyclization protocol was utilized to construct the large planar aromatic skeleton by carbon-carbon bond formation. The oxidative cyclization reaction proceeded slower because of the polar TEG chains, and was accomplished overnight at room temperature to afford **1** in 85% yield.^[9] In our modular approach, the peripheral substituted group can be easily altered, and thus the intermolecular interactions and electronic characteristics of the target molecules can be precisely tuned. Compound **1**, which is a pale-yellow solid, is readily dissolved in common organic solvents, such as CHCl_3 , CH_2Cl_2 , THF, and toluene. The structure and purity of all compounds were verified by ^1H and ^{13}C NMR spectroscopy and high-resolution mass spectrometry. The thermal decomposition temperature of 400°C under a nitrogen atmosphere revealed a good thermal stability of **1** (Figure S3 in the Supporting Information).

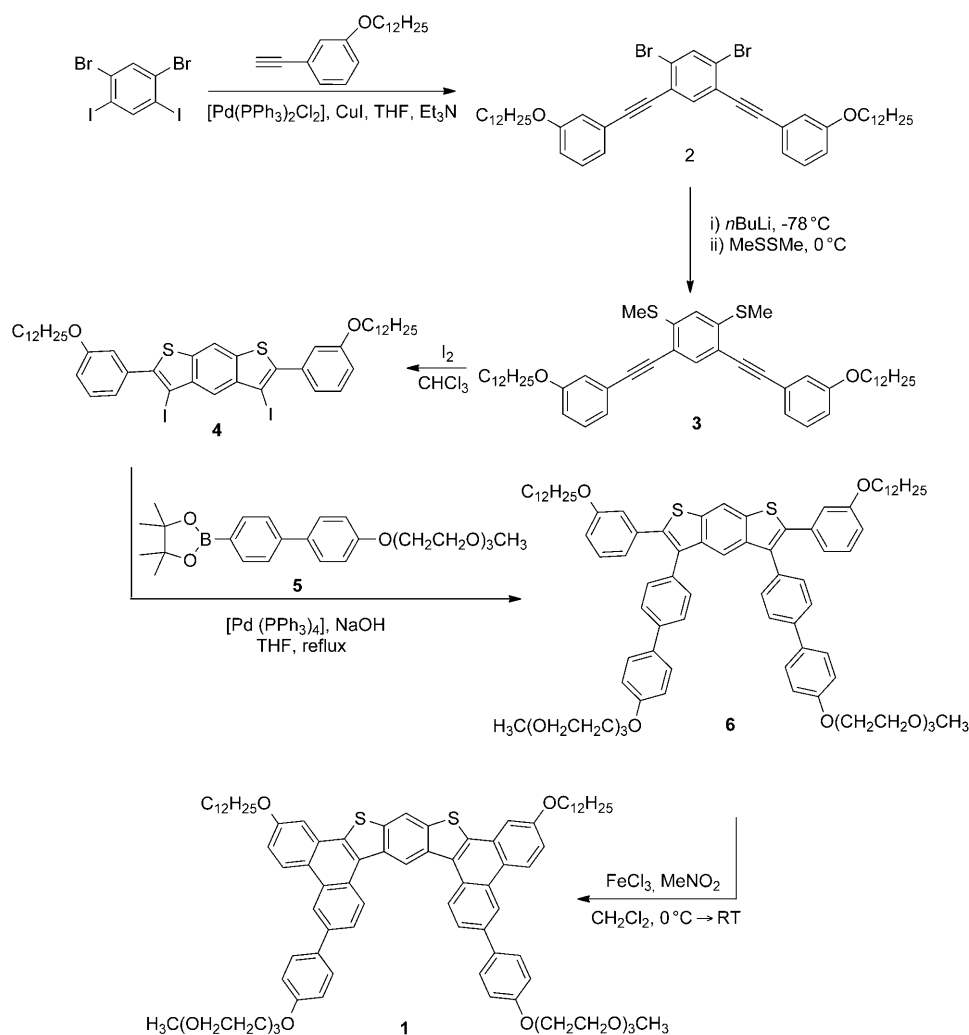
The self-assembly of **1** was performed by a common heating-cooling process. Compound **1** (5 mg) was suspended in $\text{CHCl}_3/\text{MeOH}$ (1:2 v/v, 3 mL) and heated to 50°C . A clear solution was obtained and filtered with a $0.2 \mu\text{m}$ filter. Precipitates were formed from the homogenous solution while it was slowly cooled to room temperature. Scanning electron microscopy (SEM) and transmission electron microscopy (TEM) were employed to investigate the morphology of the precipitates. As shown in Figure 1 a, b, 2D filmlike assemblies were formed. These assemblies can grow as large as $50 \mu\text{m} \times 50 \mu\text{m}$ (Figure S1 and Figure 1 a), and have high surface area, thin thickness, and good flexibility. The sheetlike assemblies show obvious birefringence under polarized optical microscopy (Figure 1 c), which indicated that these supramolecular assemblies have highly ordered architectures. This result was also substantiated by differential scanning calorimetry (DSC) where two endothermic transitions at 40°C and 150°C were observed (Figure 1 d).

To further understand the formation process of the self-assembled 2D films, the concentration-dependent ^1H NMR spectra and photophysical properties of **1** were investigated. In CDCl_3 solution, the proton signals of **1** shifted upfield as the concentration was increased from 10^{-4} to 10^{-2} M (Figure 2 a), which is a result of the shielding effect of the ring current of neighboring aromatic molecules through a cofacial

[*] J. Yin, Y. Zhou, T. Lei, Prof. J. Pei
Beijing National Laboratory for Molecular Sciences
The Key Laboratory of Bioorganic Chemistry & Molecular
Engineering of Ministry of Education
College of Chemistry, Peking University, Beijing 100871 (China)
Fax: (+86) 10-6275-8145
E-mail: jianpei@pku.edu.cn

[**] This research was financially supported by the Major State Basic Research Development Program (No. 2009CB623601) from MOST and by the National Natural Science Foundation of China.

Supporting information for this article is available on the WWW under <http://dx.doi.org/10.1002/anie.201100712>.



Scheme 1. Synthetic route to amphiphilic molecule **1**.

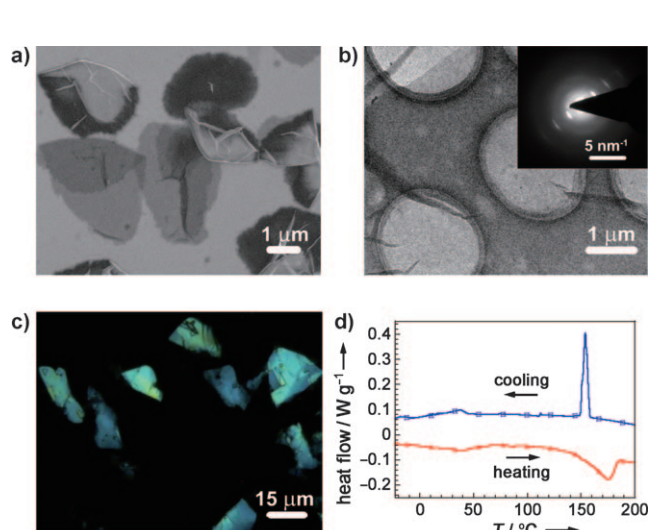


Figure 1. a) SEM image, b) TEM image (inset: corresponding SAED patterns), c) polarized optical microscopy image with cross-polarizers of sheetlike assemblies of compound **1**, and d) DSC profile of sheetlike assemblies of **1** in the first heating/cooling cycle at a rate of $10^{\circ}\text{C min}^{-1}$.

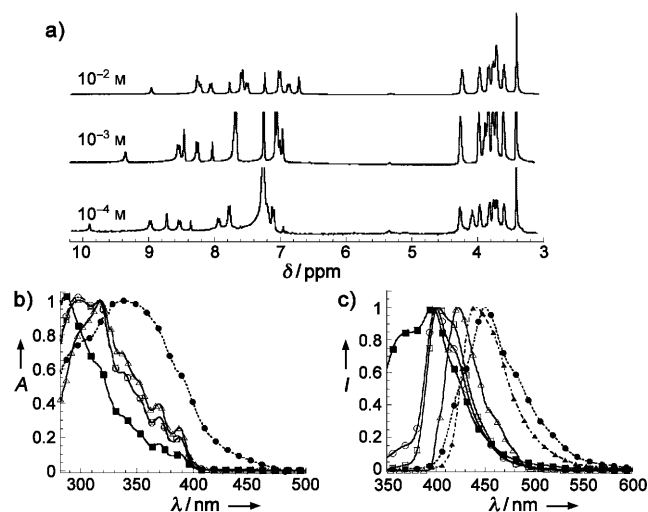


Figure 2. a) Comparison of ^1H NMR spectra of **1** at different concentrations in CDCl_3 . Changes in the b) normalized absorption and c) normalized emission spectra of **1** in CHCl_3 at different concentrations (open triangle: 1×10^{-4} M, open square: 1×10^{-5} M, open circle: 1×10^{-6} M, filled square: 1×10^{-7} M), spin-coated film (filled triangle), and precipitates (filled circle) formed in $\text{CHCl}_3/\text{MeOH}$ (1:2 v/v).

stacking.^[10] Figure 2b shows the absorption spectra of **1** in CHCl_3 solution and in the solid state. The intensities of two absorption bands at 370 and 388 nm increased as the concentration of the solution was increased, thus indicating the formation of J-aggregates because of the strong π - π stacking interactions among the conjugated skeletons.^[11] The absorption features in the drop-cast film of the aggregates displayed a broad absorption at 340 nm, which is red-shifted about 20 nm relative to that in the solution. Such behavior was observed for the emission maximum λ_{max} , which also shows a considerable red-shift when changing from solution to the solid state (Figure 2c).^[12]

X-ray diffraction (XRD) of bulky films of **1** gave well-defined diffraction patterns that are attributed to the reflections from (001) to (005) planes and suggest a typical lamellar structure (Figure 3a). The lamellar d spacing is 30.9 Å, which is about 7 Å larger than the molecular structure models (calculated

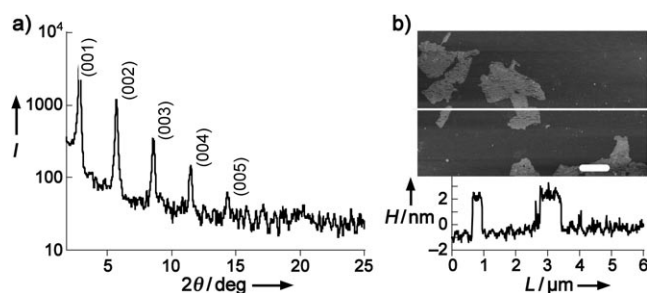


Figure 3. a) XRD patterns of the films self-assembled from $\text{CHCl}_3/\text{MeOH}$ (1:2 v/v). b) AFM image and thickness analyses of the self-assembled films. Scale bar = 1 μm .

23 Å). The image of the selected-area electron diffraction (SAED; Figure 2b, inset) exhibited a crystalline pattern with two pairs of sharp diffraction spots, (100) and (200) that correspond to a d spacing of 3.7 Å, which is a typical π – π stacking distance. The results indicated that the strong π – π stacking between the molecular skeletons is along the sheet planes, which is favorable for charge transport. Atomic force microscopy (AFM) was also employed to study the lamellar structure of the films. AFM images showed that, with the exception of filmlike assemblies with thickness in the order of hundreds of nanometers, individual thin films with a uniform height of approximately 4.0 nm could also be observed (Figure 3b), which was close to twice the length of the molecular structure (calculated 4.6 nm). In view of the molecular structure properties and dimensions of amphiphilic **1**, we proposed that the amphiphile packs into a bilayer structure, in which the hydrophobic benzodithiophene aromatic skeleton with interdigitated long alkyl chains were packed toward the interior of the film and the TEG chains were exposed to the outside. The difference of the height of the XRD and AFM measurements suggested that the alkyl chains and TEG chains are intercalated or bent in the multilayer lamellar structures. The proposed structure is illustrated in detail in Figure 4.

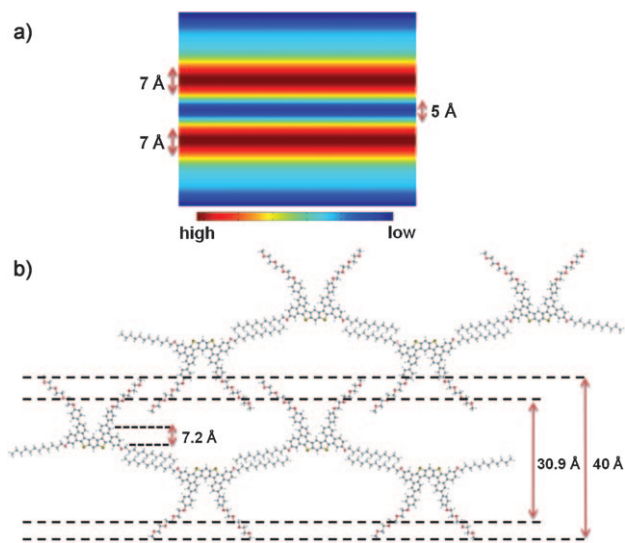


Figure 4. a) Reconstructed electron density map of self-assembled **1**. b) Proposed model of the organization of the bilayer structure of **1**.

To obtain the detailed information of the repeating unit of the lamellar structure, the intensities of the five diffraction peaks obtained from XRD data were employed to reconstruct the intralamellar electron density profiles (Table S1).^[13] As shown in Figure 4a, the high-electron-density region (shown in yellow to red) has a width of 7 Å, which is consistent with the molecular length of the fused-ring conjugated benzodithiophene skeleton region (calculated 7.2 Å). The two high-electron-density regions are flanked by the low-electron-density regions, which contain the interdigitated alkyl chains in the middle (blue band with approximate width of 5 Å) and the TEG-substituted phenyl group on the outer sides (cyan to blue; Figure 4a). The electron density profiles indicated that the parts of the alkyl chains occupy a very small region (central area, 5 Å; Figure 4a), thus implying that the alkyl chains are closely packed.

FTIR spectroscopy of the supramolecular assemblies **1** showed strong stretching vibrations of CH_2 groups at 2920 (ν_{anti}) and 2850 cm^{-1} (ν_{sym} ; Figure S2), thus contributing to the crystalline packing of the alkyl chains,^[8a,14] which is consistent with the proposed close-packing model. Based on the above results, the two phase-transition peaks observed in the DSC measurements can be explained as follows: the minor transition (40°C) was related to a reorganization of the alkyl chains from a highly ordered state to a lower ordered state, as observed in some liquid-crystalline molecules.^[15] The second main transition (150°C) was attributed to the destruction of the ordered lamellar packing and resulted in an isotropic state. Therefore, we concluded that the bilayer sheets were formed through the strong π – π stacking parallel to the surface of the films, assisted by the van der Waals interactions of long hydrophobic aliphatic chains (Figure 4b). Since the outsides of the bilayer sheets were surrounded by TEG chains, further aggregation was inhibited. Thus the resulting 2D films are free-standing, and are easily fabricated on various substrates (e.g., silicon, metal, and glass) by drop-casting or spin-coating processes.

Such free-standing films were employed as the active layer of organic field-effect transistors (OFETs). The electrodes were pre-patterned by the standard photolithographic process and followed by the thermal evaporation of titanium (5 nm) and gold (30 nm). The space between the two electrodes was 5 μm . The suspensions of the nanosheets were directly spin-coated onto an *n*-octadecyltrimethoxysilane (OTS)-treated SiO_2/Si substrate. Figure 5a shows the schematic illustration of OFETs from an individual film. Figure 5b shows a microscope image of an Au bottom-contact device constructed by a single free-standing film structure of **1**. After assembling with the free-standing films, the devices were annealed under vacuum at 70°C overnight. Typical p-channel transport characters were observed. The highest mobility was 0.02 $\text{cm}^2 \text{V}^{-1} \text{s}^{-1}$ and the on/off ratio was 10⁵. The average mobility out of 17 devices was about 0.01 $\text{cm}^2 \text{V}^{-1} \text{s}^{-1}$ and the average threshold was about 3.2 V. Figure 5c,d illustrates transfer and output characteristics of the film-based device. This is the first report of an OFET that was formed from a solution processed, self-assembled transferable free-standing film. It is also the first time that the active films were grown in solution by direct self-assembly and then transferred to the

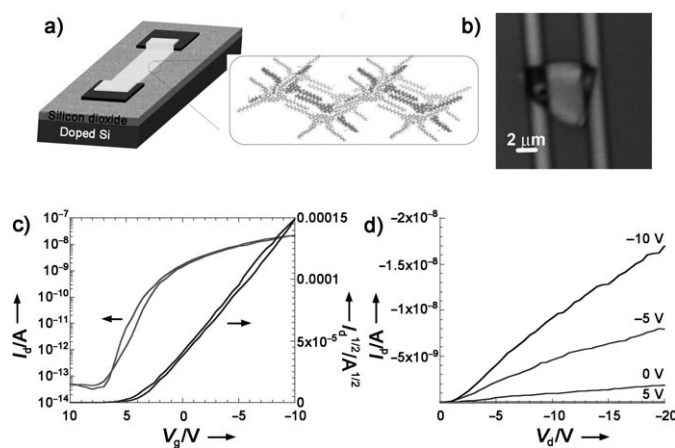


Figure 5. a) Schematic illustrations of a FET device from an individual film and the proposed bilayer supramolecular structure. b) Optical microscopy image of an individual film OFET device. c) Transfer and d) output characteristics of a 2D film transistor. The electrical characteristics correspond to the device with the best performance.

substrates. Such growth-transfer separation is the key step to break the limitation of the substrate dependence of the organic transistors.

In summary, we have developed a novel butterfly-shaped π -extended condensed benzodithiophene amphiphilic molecule **1** for organic transistors. By taking the advantage of its amphiphilic properties, this molecule easily forms 2D free-standing films by direct self-assembly in solution. The detailed characterization of the free-standing films demonstrate that a lamellar structure is formed through a bilayer arrangement. The strong π - π interactions parallel to the surface of the films not only sustain the film but also make such films electronically active. This is the first report of the use of highly ordered free-standing films to fabricate OFET devices. Organic transistors with the highest mobility of $0.02 \text{ cm}^2 \text{ V}^{-1} \text{ s}^{-1}$ have been successfully produced. Our results indicate that such an amphiphilic molecule is a promising organic 2D nanomaterial that has the predominance of large-area deposition and solution processability. Moreover, as the bilayer films are very similar to phospholipids, they hold great promise in biomembrane mimetic applications. This work is currently in progress.

Received: January 28, 2011
Published online: May 27, 2011

Keywords: amphiphiles · bilayers · free-standing films · molecular electronics · self-assembly

- [1] a) F. A. Ponce, D. P. Bour, *Nature* **1997**, *386*, 351–359; b) C. D. Dimitrakopoulos, P. R. L. Malenfant, *Adv. Mater.* **2002**, *14*, 99–117.
[2] a) Y. Ito, A. A. Virkar, S. Mannsfeld, J. H. Oh, M. Toney, J. Locklin, Z. Bao, *J. Am. Chem. Soc.* **2009**, *131*, 9396–9404; b) G. Roelkens, J. Van Campenhout, J. Brouckaert, D. Van Thour-

- hout, R. Baets, P. Rojo Romeo, P. Regreny, A. Kazmierczak, C. Seassal, X. Letartre, G. Hollinger, J. M. Fedeli, L. Di Cioccio, C. Lagahe-Blanchard, *Mater. Today* **2007**, *10*, 36–43; c) S. Mokka-pati, C. Jagadish, *Mater. Today* **2009**, *12*, 22–32.
[3] a) J. Yoon, S. Jo, I. S. Chun, I. Jung, H. Kim, M. Meitl, E. Menard, X. Li, J. J. Coleman, U. Paik, J. A. Rogers, *Nature* **2010**, *465*, 329–334; b) K. Chung, C.-H. Lee, C.-C. Yi, *Science* **2010**, *330*, 655–657; c) Q. Liu, T. Fujigaya, H.-M. Cheng, N. Nakashima, *J. Am. Chem. Soc.* **2010**, *132*, 16581–16586.
[4] a) A. A. Gorodetsky, C.-Y. Chiu, T. Schiros, M. Palma, M. Cox, Z. Jia, W. Sattler, I. Kymissis, M. Steigerwald, C. Nuckolls, *Angew. Chem.* **2010**, *122*, 8081–8084; *Angew. Chem. Int. Ed.* **2010**, *49*, 7909–7912; b) R. de Bettignies, Y. Nicolas, P. Blanchard, E. Levillain, J.-M. Nunzi, J. Roncali, *Adv. Mater.* **2003**, *15*, 1939–1943; c) W. Jiang, Y. Zhou, H. Geng, S. Jiang, S. Yan, W. Hu, Z. Wang, Z. Shuai, J. Pei, *J. Am. Chem. Soc.* **2011**, *133*, 1–3.
[5] a) F. J. M. Hoebe, P. Jonkheijm, A. P. Meijer, A. P. H. J. Schenning, *Chem. Rev.* **2005**, *105*, 1491–1546; b) A. L. Briseno, S. C. B. Mannsfeld, S. A. Jenekhe, Z. Bao, Y. Xia, *Mater. Today* **2008**, *11*, 38–47; c) A. Ajayaghosh, A. V. Praveen, *Acc. Chem. Res.* **2007**, *40*, 644–656.
[6] a) R. Li, W. Hu, Y. Liu, D. Zhu, *Acc. Chem. Res.* **2010**, *43*, 529–540; b) C. Reese, Z. Bao, *Mater. Today* **2007**, *10*, 20–27; c) J. Zaumseil, H. Sirringhaus, *Chem. Rev.* **2007**, *107*, 1296–1323.
[7] a) J.-H. Ryu, D.-J. Hong, M. Lee, *Chem. Commun.* **2008**, 1043–1054; b) E. Lee, J.-K. Kim, M. Lee, *Angew. Chem.* **2009**, *121*, 3711–3714; *Angew. Chem. Int. Ed.* **2009**, *48*, 3657–3660.
[8] a) J. P. Hill, W. Jin, A. Kosaka, T. Fukushima, H. Ichihara, T. Shimomura, K. Ito, T. Hashizume, N. Ishii, T. Aida, *Science* **2004**, *304*, 1481–1483; b) Y. Yamamoto, T. Fukushima, Y. Suna, N. Ishii, A. Saeki, S. Seki, S. Tagawa, M. Taniguchi, T. Kawai, T. Aida, *Science* **2006**, *314*, 1761–1764.
[9] a) Y. Zhou, W.-J. Liu, Y. Ma, H.-L. Wang, L. Qi, Y. Cao, J. Wang, J. Pei, *J. Am. Chem. Soc.* **2007**, *129*, 12386–12387; b) J. Pei, W. Zhang, J. Mao, X. Zhou, *Tetrahedron Lett.* **2006**, *47*, 1551–1554; c) Y. Zhou, W.-J. Liu, W. Zhang, X.-Y. Cao, Q.-F. Zhou, Y. Ma, J. Pei, *J. Org. Chem.* **2006**, *71*, 6822–6828.
[10] a) A. S. Shetty, J. Zhang, J. S. Moore, *J. Am. Chem. Soc.* **1996**, *118*, 1019–1027; b) Y. Hamuro, S. J. Geib, A. D. Hamilton, *J. Am. Chem. Soc.* **1997**, *119*, 10587–10593; c) S. Xiao, M. Myers, Q. Miao, S. Sanaur, K. Pang, M. L. Steigerwald, C. Nuckolls, *Angew. Chem.* **2005**, *117*, 7556–7560; *Angew. Chem. Int. Ed.* **2005**, *44*, 7390–7394.
[11] a) A. D. Schwab, D. E. Smith, C. S. Rich, E. R. Young, W. F. Smith, J. C. de Paula, *J. Phys. Chem. B* **2003**, *107*, 11339–11345; b) S. Yagai, T. Seki, T. Karatsu, A. Kitamura, F. Würthner, *Angew. Chem.* **2008**, *120*, 3415–3419; *Angew. Chem. Int. Ed.* **2008**, *47*, 3367–3371; c) F. C. Spano, *Acc. Chem. Res.* **2010**, *43*, 429–439.
[12] The changes in the bands at 370 nm in Figure 2c arise from the effect of self-absorption.
[13] a) B. Chen, X. Zeng, U. Baumeister, G. Ungar, C. Tschierske, *Science* **2005**, *307*, 96–99; b) F. Liu, B. Chen, B. Glettner, M. Prehm, M. K. Das, U. Baumeister, X. Zeng, G. Ungar, C. Tschierske, *J. Am. Chem. Soc.* **2008**, *130*, 9666–9667.
[14] G. John, M. Masuda, Y. Okada, K. Yase, T. Shimizu, *Adv. Mater.* **2001**, *13*, 715–718.
[15] a) X. Feng, W. Pisula, M. Takase, X. Dou, V. Enkelmann, M. Wagner, N. Ding, K. Müllen, *Chem. Mater.* **2008**, *20*, 2872–2874; b) C.-Z. Li, Y. Matsuo, E. Nakamura, *J. Am. Chem. Soc.* **2009**, *131*, 17058–17059.